DEFORMATION OF SMALL CIRCULAR UNDERGROUND OPENINGS
PART IV. BEHAVIOUR DURING FAILURE

P.K. Kaiser *
A. Guenot**
N.R. Morgenstern *

* Professor of Civil Engineering, University of Alberta
Edmonton, T6G 2G7 Canada

** former Graduate Student at The University of Alberta, now with
Société Nationale Elf-Aquitaine (Production), 64018 PAU CEDEX,
France

Submitted for publication to the International Journal of
Rock Mechanics and Mining Sciences and Geomechanics Abstracts

August, 1984

ABSTRACT

Tests on small circular openings have been conducted to investigate the deformation processes near tunnels at large depth or in weak rock. The test equipment has been described in Part I, typical test results documenting the behaviour of small tunnels in a jointed rock mass with time-dependent strength and deformation properties have been presented in Part II, and the pre-failure behaviour of these tunnels has been investigated in Part III. In this fourth part, results from one specific test are used to discuss the behaviour of openings in a jointed rock mass during the failure process. The test results show that it is necessary to differentiate between two modes of behaviour, yielding and rupture, if overstressing of the rock mass near the opening occurs. The observed rock mass displacements and wall convergences are compared with predictions made by one analytical and one numerical model. It is concluded that existing design models do not satisfactorily simulate the transition from yielding to rupture and that both behaviour modes must be evaluated separately for proper tunnel design and selection of optimum construction techniques. Practical implications for tunnel monitoring and interpretation of oil well breakouts are also discussed.

INTRODUCTION

During the construction of underground openings, such as tunnels, shafts, caverns and even deep boreholes for oil wells, it is often not possible to prevent stress concentrations near these openings in excess of the strength of the rock mass. Overstressed and yielding ground must therefore be accepted and considered for the selection of the most appropriate construction technique and for the design of the required support system, because uncontrolled yielding of the rock mass, for example near a tunnel, may lead to unsafe conditions or uneconomic tunnel support requirements if excessive ground loosening is permitted. Similarly, breakouts or ruptures of the wall of boreholes drilled for hydrocarbon exploration may create mud control problems, increase drilling time, sometimes drastically, and consequently lead to unnecessary expenses. Even though these stability problems are widely encountered, the mechanisms and processes controlling the occurrence of instabilities and the transition from stable to yielding and later to ruptured ground are poorly understood because it is seldom possible to make qualitative observations in sufficient detail to permit a comprehensive evaluation of the actual failure mechanisms. Hence, it is necessary to conduct laboratory tests to simulate the relevant processes in a manner that permits collection of sufficient data for a conclusive interpretation.

Guenot (1979) has conducted tests on small circular openings in samples of jointed coal to investigate the initiation and propagation of yield zones up to rupture of the wall of the

openings. The experimental facilities and the data handling procedures were presented in Part I (Kaiser and Morgenstern, 1981a) and some typical data was summarized in Part II (Kaiser and Morgenstern, 1981b). The time-independent and time-dependent prefailure behaviour was discussed in Part III (Kaiser and Morgenstern, 1982). The data presented in this final part are from one specific test (MC-4) where a complete transition, from elastic behaviour, to initiation and propagation of *yielding*, to *rupture* with ultimate tunnel wall collapse, was observed. In this fourth part, the recorded deformation measurements will be employed for the purpose of qualitatively describing the process of instability and to emphasize the difference between *yielding* and *rupture* of an underground opening. *Yielding* occurs with the onset of inelastic behaviour and is generally associated with the initiation and stable propagation of cracks or fractures. *Rupture* occurs during yielding if a mode of instability is reached locally, for example, by slip along a newly created, continuous shear surface or by buckling or spalling of thin and relatively stiff layers of rock. It often terminates in a rupture zone with directional patterns. This differentiation of failure modes is of practical significance because yielding can or must be tolerated during construction of a tunnel while rupture should be prevented for safe and economic tunnelling. Rupture occurs at high strain levels and is a particularly interesting concept for the evaluation of borehole breakouts (Bell and Gough, 1979; Bluemling *et al.*, 1983).

Following a qualitative description, the observed behaviour of the rock mass and the performance of the opening will be compared with predictions from commonly used analytical and numerical models to reach the main objective of this paper outlined below. The design of underground openings must often be based on simplified design models that assume certain fixed modes of behaviour (i.e., elasticity, plasticity or limit equilibrium models). Hence, it is important for a designer to distinguish between these modes of behaviour and to understand the different deformation processes such that they can be recognized in the field, monitored properly, and implemented correctly into a rational design technique. Underground openings are often designed and constructed following the concepts of the observational design approach (Peck, 1969) whereby comparisons are made between measurements and forecasts from either empirical guidelines or predictions made by analytical or numerical models. Knowledge of the most likely deformation or rupture mechanisms is required for the selection of the appropriate design model. More importantly, it is necessary for a proper design to verify the assumed failure process unless the most conservative assumption for a solution on the safe side has been made. The authors believe that many current attempts of back analysis from *in-situ* monitoring data often do not consider the real mechanisms adequately and hence may lead to inappropriate design conclusions.

In brief, the three main objectives are:

1. Presentation of sufficient data from one process simulation

test to describe the failure process of an opening in brittle, jointed rock and to explain the difference between yielding and rupture.

2. Demonstration of the limitations of some analytical and numerical models, commonly adopted to simulate the behaviour of openings in overstressed, brittle rock (both selected models assume correspondence of onset of yielding and rupture for the constitutive relationships).
3. Discussion of practical implications of the above with respect to two areas of application, tunnelling and deep borehole stability, as a guide for practicing engineers.

PRESENTATION OF TEST RESULTS OF TEST MC-4

The test configuration, the sample preparation techniques and the instrumentation have been described in detail in Part I (Kaiser and Morgenstern, 1981a) together with an explanation of the procedure used for the processing of the test results. A sample of regularly jointed coal (Test No. MC-4) with time-dependent strength and deformation properties (Kaiser and Morgenstern, 1981a; Kaiser and Maloney, 1982) was tested over a period of two months. First, the sample was repeatedly loaded by an isotropic stresses field (N=1) to approximately 10 MPa in order to assess the deformation properties and their distribution within the sample (Test MC-4.1). Second, a circular opening, 152 mm in diameter, was excavated in the center of the unloaded sample, then loaded by application of a nearly isotropic stress field at the boundaries of the sample, in the plane perpendicular

to the axis of the opening. Plane strain conditions were maintained by gradual application of longitudinal stresses to zero strains parallel to the opening axis. The sample was instrumented with 16 extensometers located on two concentric rings, schematically shown in Fig. 1, at r/a = 1.46 and 1.98 (± 0.06) with a tunnel radius 'a' of 76 mm and a distance 'r' to the center of the extensometer measuring range (54 ± 8 mm in length). The convergence was recorded in four directions, parallel to the major principal field stresses (A and B) and at 45° to them (C and D). The loading sequence, presented in Fig. 2, consisted of two multi-stage creep tests MC-4.2 and MC-4.3 with six creep stages each. The duration of each creep test was about one day and the field stress ratio N was kept close to unity (N = 1.08 and 0.98) to simulate an isotropic stress field.

This particular test was characterized by a visually detectable rupture of the tunnel wall during creep at 13.3 MPa (Test MC-4.2). Propagation of this rupture zone slowed down rapidly after 28 hours of creep under constant field stress and the sample could be further loaded to the final stress level of 16 MPa. Plate 1 illustrates the shape of and material distribution in the mirror-symmetric rupture zone after unloading of the sample (see also sketch in Fig. 7). After unloading of the sample the loose, broken material in the rupture zone was removed from the tunnel. The shape of the 'cleaned out' tunnel is shown in Fig. 1 together with the approximate extensometer locations and instrument numbers. The sample was then reloaded during Test MC-4.3 to observe when and to what extent rupture would propagate

if the rock mass was no longer confined by broken rock. Some indication of yielding during reloading (MC-4.3) was observed at 11 MPa and rupture propagation terminated at this and the following stress level (16.0 MPa).

Convergence Measurements

The convergence measurements of the four diameters recorded during first loading (Test MC-4.2) are presented in Fig. 3. Several observations are of interest:

1. Only minor deviations from linearity, due to crack closure at low stress levels and viscous creep during one-day creep tests, are observed up to field stresses of 13.3 MPa. The opening behaves more or less as expected for a circular opening in an isotropic material under an isotropic stress field (deviations of ± 0.1% at 13 MPa).
2. Tunnel wall rupture was visually observed at 13.3 MPa at an average tunnel closure or tangential strain of about 2.4%. This is significantly more than the failure strain of between 0.6 and 1.5% recorded during uniaxial compression tests on coal at low confining pressures. Axial failure strains of 2.4% or more were only measured during triaxial tests at confining pressures between 6 and 10 MPa (Guenot, 1979). Furthermore, the predicted tangential stress (26.6 MPa) at the wall of an opening in elastic rock at this stage is approximately 2.2 to 3.3 times the unconfined uniaxial compressive strength of the jointed coal (Kaiser and Morgenstern, 1981a).

3. Rupture initiation (at 13.3 MPa) is accompanied by a two to threefold increase in creep closure without a pronounced anisotropic deformation pattern. The least closure is recorded perpendicular to jointing and close to the area where rupture was initiated (near D).
4. Even though the evolution of the rupture zone is almost mirror-symmetric and propagates in the direction perpendicular to jointing (D), the final tunnel closure u/a at 16 MPa is fairly uniform at about 6.3 ± 0.7%. However, the large irreversible and strongly non-axisymmetric tunnel wall closure recorded after unloading indicates that plastic straining must have occurred in a non-uniform manner. The smallest nonrecoverable closure of 1.3% was observed parallel to jointing, in the direction perpendicular to the propagation of the rupture zones, where no rock mass disintegration or dilation was noticed. Almost no recovery occurred parallel to the propagation of the rupture zone.

The same information is also presented later in Fig. 7 where the tunnel convergence is normalized to the extrapolated convergence predicted for elastic rock.

Radial Strain Measurements

The extensometer measurements taken during the loading of the sample without a tunnel and a comparison of extensometer readings before and after tunnel excavation were used to determine the elastic properties of the coal in the manner described by Kaiser and Maloney (1982). From tests on Sample MC-4

it was found that the Poisson's ratio increased during loading from very low values at low field stress levels to about 0.2 at 12 MPa and that the Young's modulus varied between 1.4 and 2.2 GPa.

Radial strains measured during loading of the tunnel in Test MC-4.2, before large strains developed during rupture at 13.3 MPa, are reported in Fig. 4. The dashed line represents the average radial strain response during loading of the sample without a tunnel (compare with Fig. 8). At 13 MPa, the average radial strain with a tunnel is 0.52% less than without a tunnel. Only extensometers 15 and 16 differ significantly from this average trend, indicated by the dotted line. This deviation is most likely a result of local stiffness variation in the coal.

From the tunnel closure records in Fig. 3, it can be detected that the rupture process is time-dependent. First, rupture initiated at 13.3 MPa, or shortly before reaching this stess level, causing increased creep deformations at the following creep stage and, second, propagation of the rupture zone due to incremental loading to 16 MPa produced extremely large time-dependent tunnel convergences at this final stress level. The radial strains of 11 extensometers, recorded during these rupture propagation processes, are summarized in Figs. 5a and b for the two stress levels at 13.3 and 16.0 MPa. They provide further insight into the rupture sequence and its spatial distribution (The scale of the strain axis differs between each graph; see Fig. 1 for numbering of extensometers). Rupture initiation must have occurred at or before 13.3 MPa on one side

of the tunnel only, near Extensometer 14 (see Fig. 5a). This caused some time-dependent stress redistribution with minor straining of the rock mass near the other extensometers. At 16 MPa, this rupture zone propagated while rupture was initiated on the opposite side of the tunnel near Extensometer 16. This second rupture zone propagated toward Extensometer 12 and did not terminate before the end of the test after 23 hours. Related stress redistribution away from the rupture zone created smaller, but increased, time-dependent radial strains at extensometer locations near the rupture zone (Fig. 5.c).

QUALITATIVE EVALUATION OF TEST RESULTS

Frequently, and especially in the case where spalling (or rupture) is observed visually, the performance of tunnels or boreholes is first compared with predictions made by assuming linear elastic material response. Accordingly, for a circular opening in an isotropic material and isotropic stress field, initiation of failure would be predicted for a stress level equal to one half of the unconfined compressive strength, σ_c, of the rock mass (for the test material σ_c = 8 to 12 MPa; Kaiser and Morgenstern, 1981a). Hence, yielding should be initiated at 4 to 6 MPa. Considering possible size effects, this corresponds reasonably well with the first deviation from linearity between 5 and 7 MPa (Fig. 7). However, no visually detectable disruption of the tunnel wall was observed until loaded to 13.3 MPa, more than twice (2.2 to 3.3 times) the predicted stress level for overstressing of the rock matrix. After initiation, the rupture

zone propagated rapidly to a depth of 1.65 times the tunnel radius at a stress level only 20% higher (2.65 to 4 times the predicted initiation level).

These results agree with observations from hollow cylinder test (Simonyants *et al.*, 1970) where rupture was initiated at stress levels between 2.0 and 4.2 times the unconfined compressive strength of the test material. For an explanation of this apparent discrepancy, it is important to differentiate clearly between *yielding* and *rupture*. During a uniaxial test on a brittle material (Fig. 6.a), yield and rupture points are almost identical, that is, yield limit σ_Y and stress at rupture initiation σ_R (peak strength) are nearly equal. Normally, this equality of yield and rupture stress is adopted for analytical or numerical modelling even at higher confining pressures where σ_Y and σ_R no longer correspond (Fig. 6.a, line with long dashes; i.e., Daemen, 1975, and both models presented later). However, the test results presented in Fig. 3, schematically shown in Fig. 6.b without creep stages, demonstrate that initiation of yielding and rupture of the tunnel wall do *not* occur simultaneously (see also Fig. 7). *Yielding* starts if the tangential stress near the wall exceeds the unconfined compressive strength of the rock and continues to propagate, even in a relatively brittle material, as long as continuity is maintained in the yield zone. *Rupture* is controlled by the stored energy distribution around the opening that is dominated by heterogenerities in the rock mass. Hence, rupture will not prevail unless mechanisms arise for slip along local planes of weakness or for buckling of unconfined rock

slabs. Natural materials are always heterogeneous and it must therefore be expected that yielding will be followed by rupture. In Test MC-4, mirror-symmetric rupture occurred in an isotropic stress field because of regularly distributed discontinuities while in subsequent tests on specimens with less regular joint patterns mostly non-symmetric rupture zones developed. The stress level corresponding to the tunnel wall rupture initiation point is extremely variable. It depends on the type and areal distribution of structural weaknesses. These weaknesses seem, however, to dominate only after significant strain accumlation (in excess of uniaxial failure strains).

Disregarding this difference between yielding and rupture may lead to misinterpretation of field observations or to unacceptable simplifications. This can best be demonstrated with reference to the example of borehole breakouts and their interpretation. Bell and Gough (1979) and many since then (i.e., Bluemling *et al.*, 1983) relate the orientation of oil well breakouts exclusively to the orientation of the principal crustal stresses based on the assumption that breakouts are initiated at the point of highest tangential stress concentration (linear elastic model) and then propagate radially in the direction of the minor principal stress. The data presented from Test MC-4 clearly demonstrate that mirror-symmetric breakouts can exist in an isotropic stress field and that it is not acceptable to assume that rupture is initiated if the elastic limit is reached. An axi-symmetric yield zone may first develop in a stable manner under isotropic stresses (Fig. 6.b) until rupture is initiated

locally in a zone of weakness (or by external disturbance) and then propagates to form a rupture zone of different extent and non-circular shape. This mechanism corresponds with the process observed during Test MC-4 and supports the explanation of rock structure or rock fabric dependent borehole breakouts proposed by Babcock (1978).

At present, it is not possible to relate the orientation of breakouts to the orientation of principal stress or rock fabric exclusively because the interaction of stress induced yielding and rock structure dominate rupture. Only a consistent orientation of breakouts in various rock fabrics and in zones of sufficient areal extent may reflect a regional anisotropy in stress field. Further investigations are required to determine the interaction between orientation of stress, planes of weakness and breakouts. Research is also necessary to gain a better understanding of the rupture mechanisms and the stress level required for their initiation.

The formation of an ISRM-Commission on "Rock Failure Mechanisms in Underground Openings" (Chairman: V. Maury, France) demonstrates that this distinction between yielding and rupture of openings is of more than academic interest. For example, Maury (1977) reported of stable, unlined caverns in chalk that were excavated in a stress field exceeding the unconfined strength of the rock. Neither the experimental shaft and tunnel nor the caverns experienced major instabilities immediately or long after excavation. On the other hand, in underground openings with heavy rock busting it can often be observed that bursting occurs only

locally or that variable degrees of fracturing can be related to the extent of rock slabs. This indicates that rupture is dominated by local weakness or heterogeneities.

DATA INTERPRETATION BY ANALYTICAL MODEL

Predicted Behaviour

It is common practice to compare the performance of underground openings with analytical solutions (AFTES, 1983; Seeber and Keller, 1979; etc.). The test conditions with a circular opening under an isotropic stress field lend themself especially well for such a comparison. Many classical solutions are available for the problem of tunnel excavation in a prestressed medium (Egger, 1973; Daemen, 1975; Panet, 1976; Ladanyi, 1974; and others) but, for the interpretation of the test results, the analytical solution had to be rederived to take into account the effect of external load application. The complete derivation of the extent of the plastic zone, the tunnel convergence and the radial rock mass strains was presented by Guenot (1979) and is briefly summarized in the Appendix. This derivation follows the approach adopted by Panet (1976) for a material with a linear peak and ultimate (residual) Mohr-Coulomb failure criterion each described by two parameters c and ϕ. The brittleness of the rock mass is characterized by a parameter s (s = ratio of ultimate to peak strength) and the volume change properties during yielding due to dilation by a factor α.

The predicted total tunnel convergence, normalized to the elastic tunnel convergence, is plotted in Fig. 7 for three brittleness parameters (s = 1.0, 0.8 and 0.6) as a function of the applied, isotropic stress σ_o. The strength parameters listed in this figure correspond to our best estimates (based on laboratory testing) of typical average properties of the rock mass. The magnitude of the dilation parameter (a = 3) was chosen to simulate an upper limit of dilation following the associated flow rule. Other cases were analyzed by Guenot (1979) but this is the most appropriate assumption for yield zones 'R' of limited extent (see sketch in Fig. 7; R/a = 1.25 to 1.41 for s = 1.0 to 0.6).

The average radial strains, calculated based on the same analytical model, are presented in Fig. 8 for comparison with the actual measurements (Figs. 4 and 8). The extensometer anchor points are installed at 10 and 60 mm from the tunnel wall corresponding to an average anchor point located at r/a = 1.46 for the inner ring of extensometers. The predicted strains for this location and for a linear elastic, with and without tunnel, and for an elastic-brittle plastic rock are shown (s = 1.0 to 0.6).

Comparison with Observed Behaviour

The predicted difference between radial strains near a tunnel in an elastic medium with and without tunnel of 0.5% compares well with the observed, average difference of 0.52% (Fig. 4).

Individual convergence measurements of four diameters (A) to (D) and the average of the range are shown on Fig. 7. Because of the incremental loading sequence with stage creep tests, several assumptions had to be made for the determination of these normalized tunnel convergence curves: (a) only the measurements at the end of the creep stages were considered and thus reflect the longterm behaviour of the tunnel; and (b) the elastic tunnel convergence for the normalization was calculated assuming E = 1.0 GPa (lower bound of measured longterm modulus) for longterm behaviour and Poisson's ratio υ = 0.2. To eliminate the effects of crack closure at low stress levels, it was assumed that this elastic response was only reached at the end of the creep test at 5 MPa.

Non-elastic tunnel convergence was predicted and first observed by one convergence gauge at 7 MPa. At the following stress level all four convergence gauges deviated from linearity and the average convergence followed exactly the curve predicted for an elastic, perfectly plastic material (s = 1.0) up to rupture initiation and then deviated sharply after rupture had propagated. During yielding (<13.3 MPa) a more or less isotropic deformation pattern can be observed from these convergence measurements and from the radial strain measurements (Fig. 4). However, after initiation of rupture an anisotropic behaviour is apparent with a maximum convergence perpendicular to jointing due to dilation in the rupture zone, and less convergence in the areas where no or little disruption of the rockmass was detected. The opening deformed similar to an elliptical opening, with the

short axis parallel to the direction of jointing, in an isotropic stress field. While the relatively large convergence at (D) and possibly (B) is caused by dilation, the large increase in convergence for the other two diameters must be attributed to a change in effective opening geometry because little dilation could be noticed in these directions (A and C). This interpretation is also confirmed by the response of the opening during unloading (Fig. 3). Most of the convergences (A) and (C) were largely recoverable while no recovery occurred near the rupture zone (B and D). Furthermore, there is an obvious discrepancy between the extent of the predicted circular yield zone (Fig. 7, top sketch) and the observed behaviour with a mirror-symmetric rupture zone and no visually detectable distress near (C).

Comparison of the predicted radial strains (Fig. 8) and the observed strains before rupture (up to 13.3 MPa, Fig. 4) as well as after rupture (for two typical extensometers 13 and 14 up to 16 MPa, Fig. 8) leads to the same interpretation. First, the fact that no extension and fairly uniform straining was recorded below 13.3 MPa confirms the earlier finding of isotropic elastic, perfectly plastic yielding with no or little strength loss (s = 1.0) before rupture initiation. Second, the non-axisymmetric nature of the rupture propagation process is clearly reflected by the two examples of Extensometers 13 and 14 (Fig. 8). While No. 14 records extensional strains far beyond those expected for a yielding and dilating material, No. 13 shows little extension and, hence, lies outside the rupture zone and most likely outside

the yield zone.

At rupture there is a discontinuity in the slope of the convergence curve (Fig. 6.b). The observed convergence after rupture could certainly be matched by a perfectly brittle, plastic model but the required peak strength would be in excess of the actual strength and the resulting shape and extent of the yield zone would not correspond with the observed rupture zone. Alternatively, if the correct peak strength is assumed, the observed discrepancies can only be explained by a different post-yield behaviour as indicated by the line with short dashes in Fig. 6.a. The observed convergence could be matched in this fashion but the shape and extent of the rupture zone would still differ from the observed.

In summary, the analytical model confirms the findings of the qualitative interpretation. It is capable of describing the onset and propagation of yielding but does not anticipate the onset of rupture. This obvious limitation of the analytical model must be respected during its application to the interpretation of field measurements. For example, in Test MC-4 this model cannot be used to explain the final convergence at 16.6 MPa and hence the ultimate tunnel behaviour. Only recognition of the actual rupture mechanisms permits, at least qualitatively, interpretation of the excessive convergence parallel to jointing or in the direction of stable ground. Similar conditions may be encountered near real underground openings in overstressed rock, where the occurrence of rupture is not easily detectable. Blind applications of these anlaytical models beyond the rupture point

leads to wrong and most likely dangerous interpretations of the actual ground conditions.

DATA INTERPRETATION BY NUMERICAL MODEL

Predicted Behaviour

Many more or less sophisticated numerical models are available for the simulation of openings in brittle, jointed rock. It is not possible, or intended, to present here a complete evaluation of these models. However, considering the anisotropic strength of a regularly jointed material, it seems appropriate to introduce at least this aspect in a model and to compare predicted and observed opening response. For this purpose, a finite element analysis was carried out assuming that the rock mass would behave like an elasto-plastic material with anisotropic strength characteristics. One of the main requirements of the finite element model described below is continuity, that is, slip along planes of weakness induce continuous anisotropic yielding but the rock mass maintains compatible deformations. Since it was the purpose of this investigation to establish whether the mode of behaviour could be modelled accurately only one typical set of parameters, selected to represent mean material properties, was employed to calculate the tunnel convergence, the extent of the yield zone (inside the rock matrix), the zone where slip along planes of weakness occurs, and the distribution of the tangential stresses near the tunnel wall.

The analysis was carried out with the general purpose finite element code ROSALIE of the Central Laboratory for Bridges and Roads (Paris) (Yuritzinn *et al.*, 1982) on one quarter of the sample, discretized by finite elements as shown in Fig. 9. This mesh was loaded in steps from 5 to 15 MPa by application of pressure increments of 2 MPa at the sample boundary and by maintaining plane strain conditions. Twenty iterations were executed at each stress level. The assumed, isotropic deformational properties of the elements are, Young's Modulus E = 1.5 GPa and Poisson's ratio υ = 0.2. The anisotropic strength behaviour was obtained by simultaneous consideration of the following criteria:

- Linear elastic, perfectly plastic stress strain relationship for the intact rock with a linear Mohr-Coulomb failure criterion defined by an angle of internal friction ϕ = 30° and a cohesion intercept of 4 MPa.
- Directional yield criterion to describe the strain-softening behaviour of the discontinuities, defined by a peak cohesion intercept of 1.5 MPa, an ultimate cohesion of 0.3 MPa and a constant angle of internal friction of 30°.
- Limited-tension criterion (σ_T = 1 MPa).

The strength loss along the discontinuities between peak and ultimate was assumed to be almost instantaneous and the flow rule was chosen to prevent dilation of the discontinuities. The model does not simulate distinct discontinuities but a continuous material with oriented strength, hence it is called a 'stratified material' model. The details of this material model were

described by Frank *et al.* (1982) together with a comparison of the 'stratified material' model with a model using discrete discontintuities (joint elements). They demonstrated good agreement of deformations predicted for rock masses with closely spaced joints.

The results of the numerical analysis are summarized in Fig. 10 for four stress levels. In Fig. 10.a, the extent of the plastic zone is illustrated by arrows, if yielding in an element occurred along a plane of weakness parallel to jointing, and by circles if the rock matrix reached the yield limit. Failure is evaluated at the nodal points. At 5 MPa field stress, directional failure is reached in a limited area near the tunnel wall (between B and D) but only if a discontinuity actually exists in this zone. In the event that there is no discontinuity penetrating this area, no yielding would occur and the observed deformations would be less than predicted. It is likely that no slip occurred during Test MC-4 at this stress level because no discontinuity intercepted the yield zone or because the strength of the joints was higher than assumed. At 7 MPa, first yielding of the rock matrix to a limited extent is predicted at the tunnel wall at Point (D) and near Point (C). At 13 and 15 MPa the yield zones, both in the rock matrix and parallel to the discontinuities, expand to reach an almost circular shape.

It must be noted that the stresses inside the two types of yield zones are not uniform because of the difference in the ultimate material strengths. The resulting tangential stress distribution at the tunnel wall is presented in Fig. 10.c whereby

the magnitude of the tangential stress is given by the length of the lines extending radially from the circumference of the tunnel (tensile stresses are plotted inward). Because of the relatively large elements chosen for this analysis the stresses shown in Fig. 10.c are not very accurate. Greater accuracy would only be achieved with a much finer mesh near Point (B) that would accommodate large shear strain gradients and adequately model the rapid rotation of principal stresses near the tunnel wall and near yielding planes of weakness (from σ_1 tangential to the wall to σ_1 nearly perpendicular to the yielding discontinuities). Nevertheless, Fig. 10.c demonstrates clearly that high concentrations of tangential stresses are created near Point (D) where the joints are tangential to the tunnel wall. This stress concentration influences or possibly dominates the rupture process.

The normalized radial tunnel convergence and the resulting deformed tunnel shape are presented in Figs. 11 and 10.b, respectively. At low stress levels, shear failure and displacements along discontinuities lead to a rapid increase in tunnel convergence near Point (B). After further loading to higher stress levels, the convergence increases further until a maximum is reached parallel to jointing (C) because of crushing or yielding of intact rock near Point (D) where the highest tangential stresses are predicted. Fig. 11 also contains for comparison the normalized displacements calculated by the analytical model (s = 1.0 and 0.8) and by the finite element method for an isotropic, elastic-perfectly plastic material. The

results of the finite element method deviate from the analytical results as expected because of differences in the basic assumptions, i.e., volume change relationship inside the yield zone. Nevertheless, the shape and trend is very similar. It is of particular interest to note how little deviation from uniform tunnel convergence is predicted by the 'stratified' model even though non-uniform tangential stresses and non-symmetric yield zones exist. These results clearly demonstrate how insensitive the tunnel convergence is to the shape of the yield zone, an observation that is of great practical importance.

Comparison with Observed and Analytically Predicted Behaviour

The results from the 'stratified' model provide some further insight. Initiation of yielding is predicted at 4 to 5 MPa. This does not correspond with the observations (Fig. 7), most likely because no discontinuity was intersected as assumed by the finite element analysis. However, the sequence of events corresponds extremely well with the observed. First, shear of joints is reflected by a sudden increase in convergence near Point (B) but this diameter shows a less rapid increase in convergence at higher stress levels. Yielding near Points (D) and (C) is only detectable at 1 to 2 MPa higher field stresses but the convergence increases rapidly thereafter. At the rupture point, at 13.3 MPa, maximum convergence is predicted (and observed) at (C) parallel to jointing. This confirms the earlier finding that the highly stressed opening behaves like an elliptical tunnel in an isotropic stress field.

Initiation of rupture and the response of the tunnel after rupture again cannot be predicted, as expected, by this finite element continuum model, but it is of interest to note that rupture was initiated at the stress level where the convergences (B and C) started to deviate more rapidly. Large differential straining at this stress level must have lead to a disruption of the continuum and, hence, to the propagation of a rupture zone. This observation is in good agreement with the concept of the extension strain criterion for fracture of brittle rock proposed by Stacey (1981).

CONCLUSIONS AND PRACTICAL IMPLICATIONS

Three main conclusions merit emphasis:

1. *Yielding* and *rupture* constitute two separate phases of the failure process of underground openings;
2. Analytical and numerical continuum models cannot predict rupture but are capable of adequately describing yielding; and consequently
3. Rupture mechanisms must be evaluated separately and confirmed in an observational manner by monitoring the performance of an opening.

These three general conclusions have significant practical implications:

1. Non-correspondence of yielding and rupture of underground openings:
   - The two processes must be considered separately for the

design of tunnels, for the selection of the proper construction techniques, and for the evaluation of field measurements. Assuming correspondence between yielding and rupture is an unacceptable simplification and may lead to erroneous designs. While yielding can be evaluated reasonably well by consideration of the global stress and rock mass property distribution, rupture is poorly understood because it is dominated by stress concentrations due to heterogeneities and local, structural features, particularly if they are not confined by non-yielding rock. Consequently, the convergence curve of an underground opening possesses a non-steady slope at the point of rupture. Knowledge of the location of this point is essential for the design of an opening but, unfortunately, it is extremely variable, difficult to predict and seldom measurable.

- The rupture process was found to be time-dependent and more readily detectable by observing creep deformations than from the instantaneous response to loading (or tunnel excavation increments). Hence, it can best be detected by comparing convergence or strain rates in similar ground conditions.
- For openings where propagation of rupture to a free boundary is impossible, rupture terminates even if the rock inside the rupture zone provides very little confinement (see Fig. 1 after reloading of 'cleaned out' rupture zone). The associated deformations may not be

acceptable in practice (5 to 7% in Test MC-4). Nevertheless, the convergence curve of such an opening is still gradually converging to a finite value even though at a much reduced rate.

- A comparison of the unconfined rock mass strength with the tangential stresses predicted from elasticity permits an assessment of the stress level for initiation of yielding only. Even in a brittle material, this does not correspond with the initiation of rupture of the opening wall. The combined effect of stress, strain and rock structure or rock fabric must be considered to evaluate rupture initiation and propagation. The implications of this conclusion for the interpretation of oil well breakouts were discussed earlier.

2. Limitations of analytical and numerical continuum models for stability evaluation of underground openings:
   - The types of analytical and numerical models, represented by two selected examples, cannot predict the rupture point but are adequate to describe yielding. For a rational design of a tunnel, rupture must be modelled separately even in apparently homogeneous ground because localized straining may lead to an alternate mode of instability. Nevertheless, more sophisticated finite element models provide improved insight into the stress and strain field and this facilitates a rational evaluation of appropriate rupture models.
   - The observed correspondence of large differential

straining with initiation of rupture during Test MC-4 seems to indicate that design against rupture should be based on limiting differential or extensional straining as suggested by Stacey (1981). During construction of a tunnel, this can be achieved very effectively by selecting the most appropriate excavation and support technique. For example, bolting of potential slip surfaces prevents large localized straining and, hence, prevents initiation of an otherwise possible rupture mode. The often observed benefit of short grouted bolts in relatively large yield zones can be attributed to this principle. These bolts prevent localization of straining inside the yielded rock mass and consequently eliminate rupture initiation processes.

- The test results provide some evidence that strain-weakening ($s < 1.0$) of rock near underground openings may not be as dominant as frequently assumed (i.e., Seeber and Keller, 1979). At least during Test MC-4, rupture occurred before strain-weakening was detectible from convergence measurements even though the accumulated tangential strains were far in excess of the strains required to reach the peak strength in an unconfined compression test of the brittle test material.
- On the other hand, the final convergence recorded at 16.6 MPa could be fitted reasonably well by assuming a material with 50% instantaneous strength loss ($s = 0.5$) but the shape of the yield zone predicted in this fashion

and the development of the convergence with increasing stress show that this model does not correspond with reality. The results from this investigation illustrate that matching of convergence measurements and predictions at only one stage is not sufficient to prove the validity of the applied analytical model. This does not imply that these widely adopted analytical models, i.e., for the convergence-confinement method, cannot be applied effectively to evaluate data from field monitoring but it demonstrates that the assumed failure mechanism must be verified by measurements in the field. Only after the applicability of the design model has been proven by appropriate field observations are extrapolations, for example for safety evaluations, acceptable.

3. Performance monitoring of underground openings:
   - The need for monitoring of underground openings can be justified for many reasons; for the determination of rock mass properties, for safety evaluation, for contractual documentation of tunnel performance, etc. In the context of the previous conclusions, monitoring is required to determine the mode of behaviour, yielding or rupture, and to verify the applicability of the chosen design model. In many published case histories this essential second step, verification of the assumed failure or yield mechanism, is unfortunately often missing. In addition, much of the field data interpretation is based on single, or at best double or triple, one-directional convergence

measurements and non-matching observations are often neglected. The results presented earlier illustrate that data interpretation based on one-directional convergence measurements only, is extremely dangerous and may lead to misinterpretation because many displacement fields and internal stress redistribution mechanisms lead to the same wall movements. A combination of multi-directional convergence and radial strain measurements by extensometers is necessary for a complete evaluation and justification of a design model.

For this purpose, well positioned radial extensometers should be employed to determine the extent of the yield zone and to localize zones of high differential straining. Because extremely large variations between individual extensometer readings must be expected in a jointed rock mass, failure modes can only be identified reliably by extensometers if they can be compared with reference performance records that reflect typical behaviour in stable areas. Large differences between radial strain measurements provide an excellent indicator for the identification of yield or rupture zones.

- Unfortunately, the most commonly applied means of monitoring tunnels, convergence, provides a rather poor indicator for stability evaluations. The test results demonstrate how insensitive the convergence is to yield and rupture processes. Only after rupture initiation, was

a clear deviation from linearity detectable and even then a conclusive interpretation from these convergence measurements alone was not possible. The effect of a change in effective opening geometry, both in size and shape, on the tunnel wall convergence is significant and cannot be neglected. As a matter of fact, the test results indicate that the geometry change due to yielding and rupture did dominate the deformation pattern more than the dilation in the yield zone. Large deformations did occur perpendicular to the direction of the rupture zone propagation (Test MC-4.2: parallel to jointing) and support measures would be wasted if installed in this stable area. In order to prevent rupture or to control propagation of the rupture zone and to stop tunnel convergence, bolting of possible shear and compressive failure zones (Test MC-4.2: perpendicular to jointing) would be required. If a stiff circular support ring were to be installed after initiation of rupture without reinforcement of the rupture zone, extremely large moments would develop even in this circular tunnel in an isotropic stress field.

The same difficulties, as encountered in the interpretation of this test, of finding the appropriate analytical or numerical model for the evaluation of field measurements exists in practice. Insufficient effort is often made to prove that the applied model corresponds to and describes correctly the physical processes that occur in reality. The content of this paper shows

that it is not adequate to match observed and predicted tunnel convergence measurements to verify an adopted design model. It is necessary in addition to gain information about the displacement field inside the rock mass.

REFERENCES

AFTES (1983). Recommendation on the utilization of the convergence-confinement method. Groupe de travail No. 7. Tunnels et Ouvrages Souterraines, No. 59, pp. 219-238.

Babcock, E.A., 1978. Measurement of subsurface fractures from dipmeter logs. American Association of Petroleum Geology Bulletin, Vol. 62, pp. 1111-1126.

Bell, J.S. and D.I. Gough, 1979. Northeast-southwest compressive stress in Alberta: evidence from oil wells. Earth and Planetary Science Letters, Vol. 45, pp. 475-482.

Bluemling, P., K. Fuchs and T. Schneider, 1983. Orientation of the stress field from breakouts in crystalline well in a seismic active area. Physics of the Earth and Planetary Interiors, Vol. 33, pp. 250-254.

Daemen, J.J.K., 1975. Tunnel support loading caused by rock failure. Ph.D. thesis, University of Minnesota.

Egger, P., 1973. Einfluss des Post-Failure-Verhaltens von Fels auf den Tunnel Ausbau. Veroeffentlichungen des Institutes fuer Bodenmechanik und Felsmechanik, Universitaet Fridericiana Karlsruhe, Heft 57, pp. 1-83.

Frank, R., A. Guenot and P. Humbert, 1982. Numerical analysis of contacts in geomechanics. 4th International Conference on Numerical Methods in Geomechanics, Vol. 1, pp. 37-45.

Guenot, A., 1979. Investigation of Tunnel Stability by Model Tests. M.Sc. thesis, Department of Civil Engineering, Univerity of Alberta, 217p.

Kaiser, P.K. and S.M. Maloney, 1982. Deformation properties of a

subbituminous coal mass. International Journal of Rock Mechanics and Mining Sciences & Geomechanics Abstracts, Vol. 19, pp. 247-252.

Kaiser, P.K. and N.R. Morgenstern, 1981a. Time-dependent deformation of small tunnels - I. Experimental facilities. International Journal of Rock Mechanics and Mining Sciences & Geomechanics Abstracts, Vol. 18, pp. 129-140.

Kaiser, P.K. and N.R. Morgenstern, 1981b. Time-dependent deformation of small tunnels - II. Typical test data. International Journal of Rock Mechanics and Mining Sciences & Geomechanics Abstracts, Vol. 18, pp. 141-152.

Kaiser, P.K. and N.R. Morgenstern, 1982. Time-independent and time-dependent deformation of small tunnels - III. Pre-failure behaviour. International Journal of Rock Mechanics and Mining Sciences & Geomechanics Abstracts, Vol. 19, pp. 307-324.

Ladanyi, B., 1974. Use of the long-term strength concept in the determination of ground pressure on tunnel linings. 3rd Congress of the International Rock Mechanics, Denver, Vol. IIB, pp. 1150-1156.

Maury, V., 1977. An example of underground storage in soft rock (chalk). Proceedings of Rockstore 1977, pp. 681-689.

Panet, M., 1976. La Mecanique des Roches Appliquee aux Ouvrages de Genie Civil, Association amicale des ingenieurs anciens de l'Ecole Nationale des Ponts et Chaussees, Paris, 235 pp.

Peck, R.B., 1969. Deep excavations and tunnelling in soft ground. Proc. 7th International Conference Soil Mechanics and Foundation Engineering, Mexico City, State of the Art Volume, pp. 225-290.

Seeber, S. and S. Keller, 1979. Beitrag zur Berechnung und Optimierung von Felsankern im Tunnelbau (Contribution to the Calculation and Optimization of Rock Anchors in Tunnelling). Rock Mechanics, Suppl. 8, pp. 59-74.

Simonyants, L.E., S.A. Kevorkov, and N.I. Fisenko, 1970. Study of the static strength of the area near the well bore in an uncased well. NEFT GAZ, No. 9, p. 45-50.

(Translated from Russian)

Stacey, T.R., 1981. A simple extension strain criterion for fracture of brittle rock. International Journal of Rock Mechanics and Mining Sciences & Geomechanics Abstracts, Vol. 18, No. 6, pp. 469-474.

Yuritzinn, T., M. Panet and A. Guenot, 1982. Analysis of tunnels in strain-softening grounds. 4th International Conference on Numerical Methods in Geomechanics, Vol. 2, p. 635-644.

APPENDIX

Analytical Model of Circular Opening in Isotropic, Elastic-Brittle Plastic Continuum (external, isotropic load application)

a) Failure criterion

The strength of the material is defined by a linear Mohr-Coulomb failure criterion

$$\sigma_\theta = m\,\sigma_r + s\,\sigma_c \qquad (1)$$

where: σ_θ, σ_r are the tangential and radial stresses in the rock mass;

m = $(1+\sin\phi)/(1-\sin\phi)$ with internal friction angle ϕ;

σ_c = unconfined compressive strength; and

s = coefficient characterizing the brittleness of the material, $0 < s < 1$.

b) Stress distribution in the plastic zone

The combination of the equilibrium equation and the failure criterion results in a differential equation, whose solution is, for the case with no support pressure:

$$\sigma_r = ((s\sigma_c)/(m-1))\,[(r/a)^{(m-1)} - 1]$$

$$\sigma_\theta = ((s\sigma_c)/(m-1))\,[m(r/a)^{(m-1)} - 1] \qquad (2)$$

This is identical to the real tunnelling case, called REALITY. Similarly, the solution for the plastic radius, which is not influenced by the boundary conditions, corresponds to the REALITY case because it was assumed that the boundaries are far enough from the tunnel:

$$R/a = \{((m-1)/(m+1))[(2\sigma_0-\sigma_c)/s\sigma_c] + 1\}^{(1/(m-1))}. \qquad (3)$$

c) Strains in the elastic zone

For the calculation of strains it is necessary to differentiate between REALITY and TEST (external loading) conditions:

$$\epsilon_r = (\sigma_0(1-2\nu)/2G) + (\sigma_0/2G)((\sigma_{rR}/\sigma_0) - 1)(R/r)^2$$

$$\epsilon_\theta = (\sigma_0(1-2\nu)/2G) - (\sigma_0/2G)((\sigma_{rR}/\sigma_0) - 1)(R/r)^2 \qquad (4)$$

PLATE — REALITY — TEST

where σ_{rR} is the radial stress at r=R.

d) Strains in the plastic zone

The strains in the plastic zone may be assumed as the sum of an elastic and a plastic part:

$$\epsilon = \epsilon^e + \epsilon^p.$$

Several hypotheses can be made for the elastic strain ϵ^e. The most common is to assume that it is constant throughout the

plastic zone and equal to the value at the elastic-plastic boundary. For the following the assumption that the elastic strains in the plastic zone satisfy Hooke's law was chosen. Hence, the elastic strains in the plastic zone are given by:

$$\epsilon_r^e = (s\sigma_c/2G(m-1))\,[(r/a)^{(m-1)}(1-\nu-m\nu)+2\nu-1]$$

$$\epsilon_\theta^e = (s\sigma_c/2G(m-1))\,[(r/a)^{(m-1)}(m-m\nu-\nu)+2\nu-1]. \qquad (5)$$

Because there is a discontinuity in the tangential stress profile across the plastic - elastic boundary, there will also be a similar discontinuity for the elastic strains. To ensure continuity of the total strains across the boundary, it is necessary to assume that the strength loss at the boundary induces immediate plastic strains at the boundary. The following boundary condition was used to get these plastic strains:

$$(\epsilon_\theta^p)_{r=R} = \sigma_c(1-\nu)(1-s)/2G\ . \qquad (6)$$

This helps to solve the following differential equation obtained from the equilibrium equation, the equations of elastic strain and a classical flow rule (see Panet (1976)):

$$d\epsilon_\theta^p/dr + \epsilon_\theta^p(1+a) = -(s\sigma_c/2G)(1-\nu)(m+1)(r/a)^{(m-1)}$$

$$\epsilon_\theta^p + a\epsilon_r^p = 0\ . \qquad (7)$$

This leads to the equation of plastic strains:

$$\epsilon^{p}_{\theta} = [(1-\nu)/2G]\,[(m+1)/(m+a)]\; s\sigma_{c}\,(r/a)^{(m-1)}\,[(R/r)^{(m+a)} - 1]$$

$$\epsilon^{p}_{r} = -a\epsilon^{p}_{\theta} . \qquad (8)$$

Addition of Eqns. 5 and 8 gives the total strains in the plastic zone, for the case of the TEST boundary conditions. To get the corresponding expression for the case of REALITY, the strain due to the loading of the block (Eqn. 4) must be subtracted.

The displacement field is then given by:

$$u_r/r = (\sigma_c/2G)\{s(r/a)^{(m-1)}\,[((m(1-\nu)-\nu)/(m-1))$$

$$+ ((1-\nu)((m+1)/(m+a))((R/r)^{(m+a)} - 1)] + (s(2\nu-1)/(m-1))$$

$$+ (1-\nu)(1-s)(R/r)^{(a+1)}\} \qquad (9)$$

and the tunnel closure by:

$$u^{ep}_{a}/a = (\sigma_c\,(1-\nu)/2G)\{s[1+((m+1)/(m+a))((R/a)^{(m+a)} - 1)]$$

$$+ (1-s)(R/a)^{(a+1)}\} . \qquad (10)$$

The closure of a tunnel under external load application in a linear elastic material is:

$$u^{e}_{a}/a = \sigma_0(1-\nu)/G . \qquad (11)$$

The total tunnel convergence normalized to the elastic convergence is then :

$$u^{ep}/u^{e} = (\sigma_c/2\sigma_o)\{s\,[1+((m+1)/(m+a))((R/a)^{(m+a)}-1)] + (1-s)(R/a)^{(a+1)}\} \qquad (12)$$

which is independent of the deformation properties of the elastic material.

* * * * * * * * * * *

Plate 1 View of unloaded sample after Test MC-4.2 showing mirror-symmetric rupture zones with rotated fragments indicating rupture mechanism.

Fig. 1 Instrument locations and extent of rupture zones after Tests MC-4.2 and MC-4.3; Extensometers 9 to 23; Convergence Gauges A to D.

Fig. 2 Loading sequence for Tests MC-4.2 and MC-4.3.

Fig. 3 Tunnel wall closure from four convergence gauges; Test MC-4.2 (Tunnel closure = convergence 2u/tunnel diameter 2a).

Fig. 4 Measured average radial strains at r/a = 1.47 recorded by first row of extensometers during Test MC-4.2 (compression positive).

Fig. 5 Time-dependent development of average radial strains measured by extensometers during Test MC-4.2 (Numbers correspond to extensometer locations shown in Fig. 1).

Fig. 6 Schematic diagram of (a) stress-strain curve from triaxial test and (b) stress-convergence curve for externally loaded tunnel.

Fig. 7 Measured and analytically predicted normalized tunnel

convergence (2u(E) = elastic and 2u(E+P) = total, elastic and plastic, tunnel convergence).

Fig. 8 Analytically predicted average radial strain development for a first row extensometer at r/a = 1.46 (three brittleness factors s = 1.0, 0.8 and 0.6) and measured radial strains of Extensometers 13 and 14.

Fig. 9 Finite element mesh.

Fig. 10 Results from finite element analysis:
(a) extent of plastic zone (arrow = yield of plane of weakness; circle = yield of intact rock);
(b) deformed shape of tunnel wall; and
(c) tangential stress at tunnel wall.

Fig. 11 Normalized tunnel convergence calculated by finite element method for isotropic, elastic-perfectly plastic and 'stratified material' model (also shown is relationship predicted by analytical model as in Fig. 7).

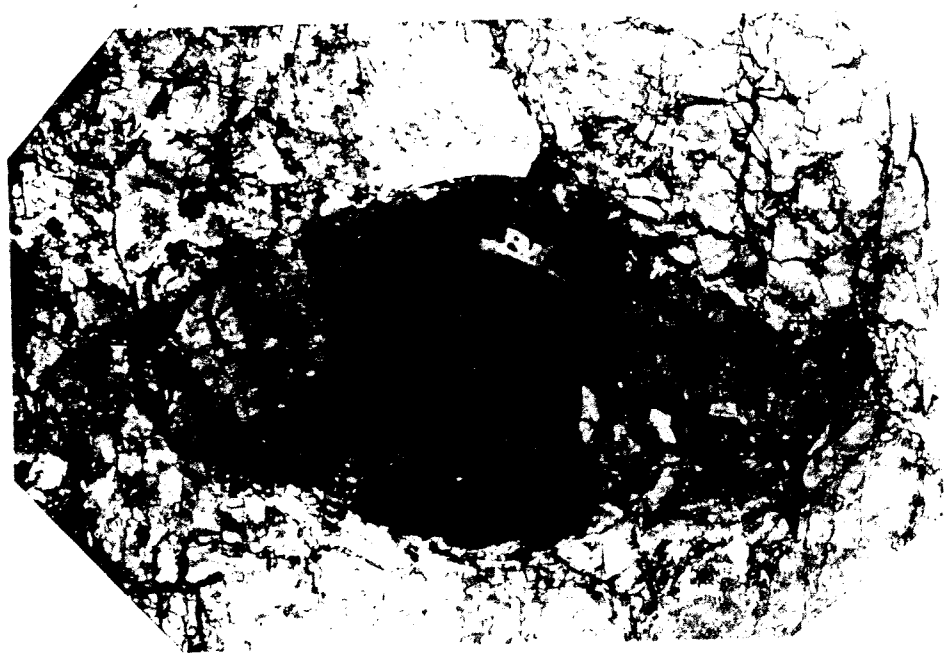

Plate 1

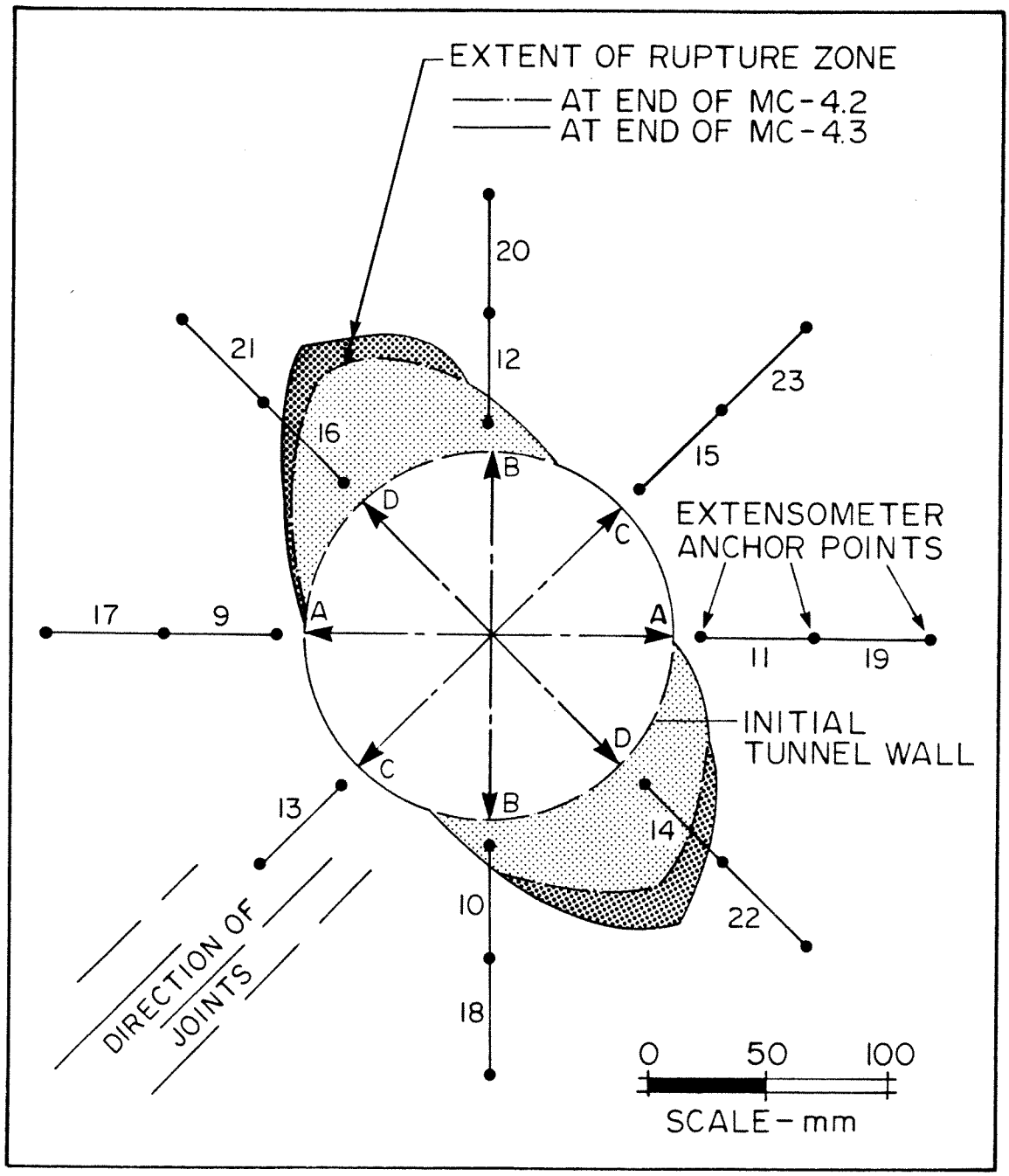

Fig. 1

Kaiser et al., 1984

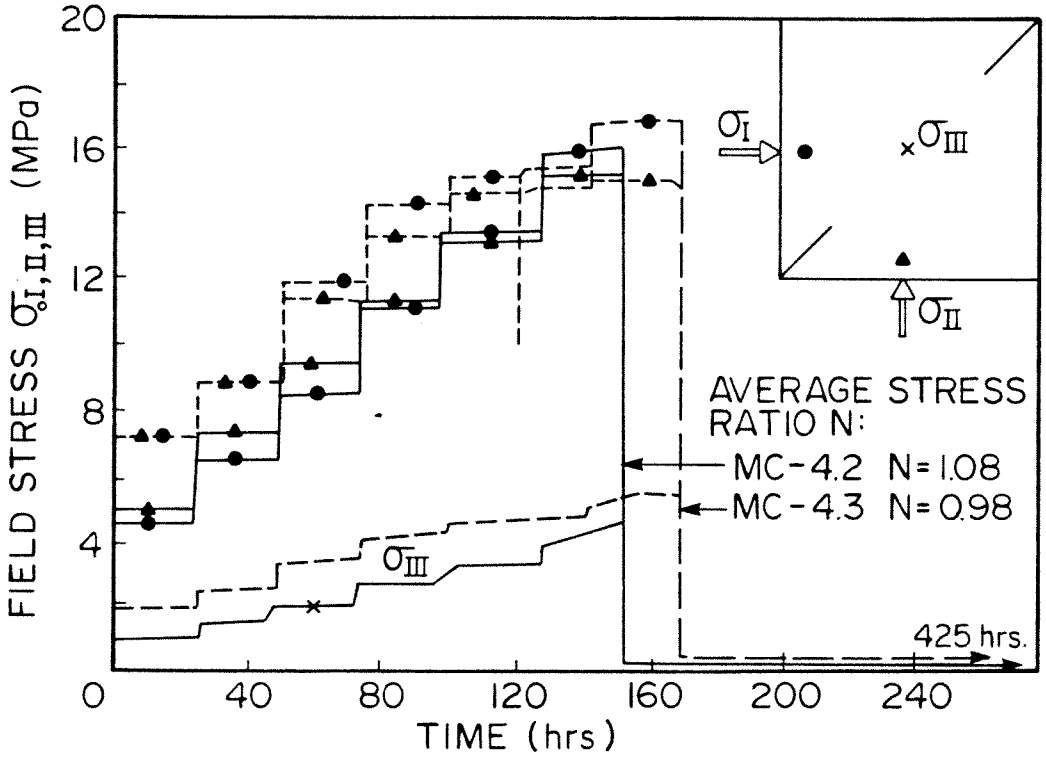

Fig. 2

Kaiser et al., 1984

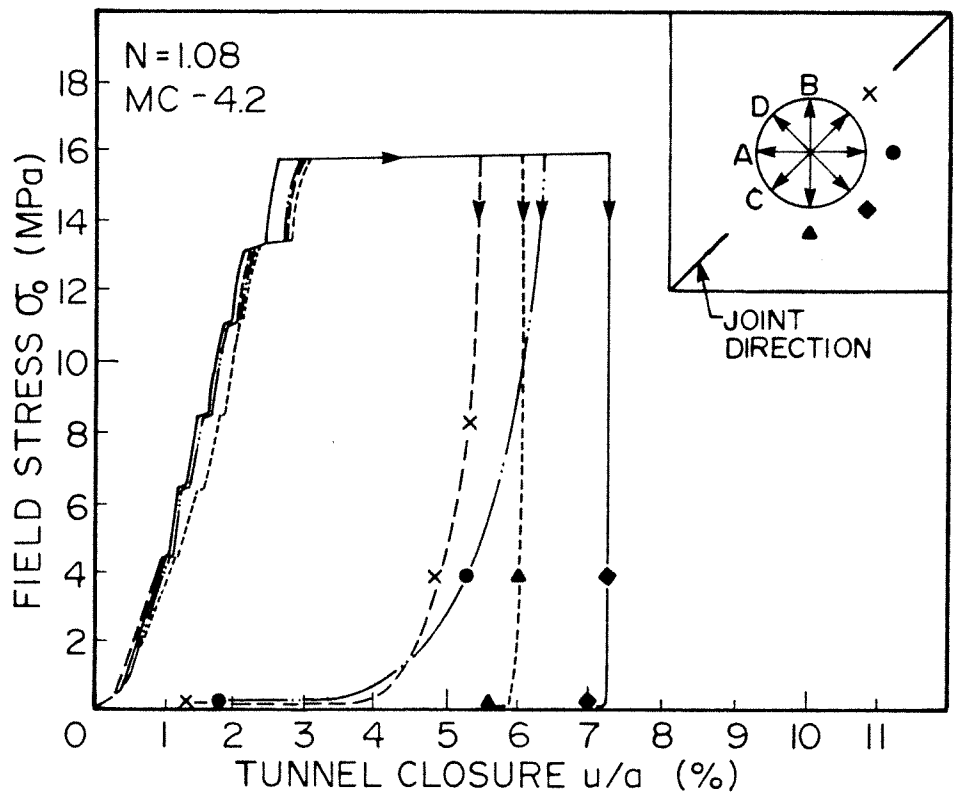

Fig. 3

Kaiser et al., 1984

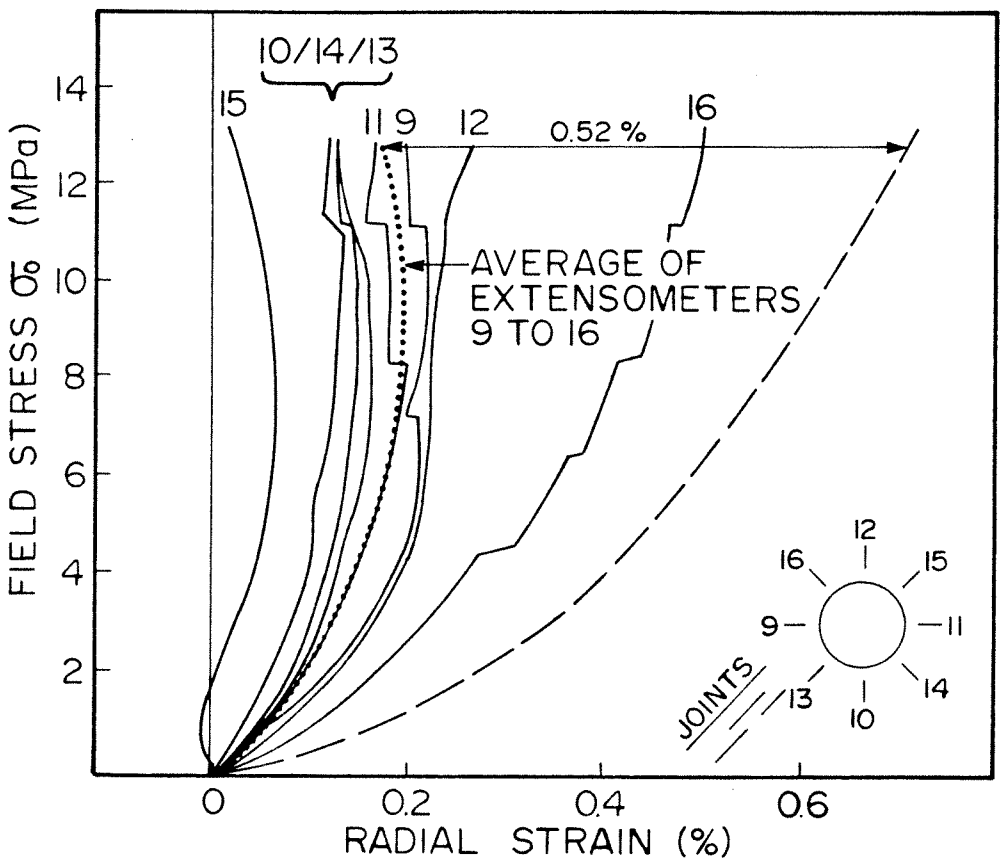

Fig. 4

Kaiser et al., 1984

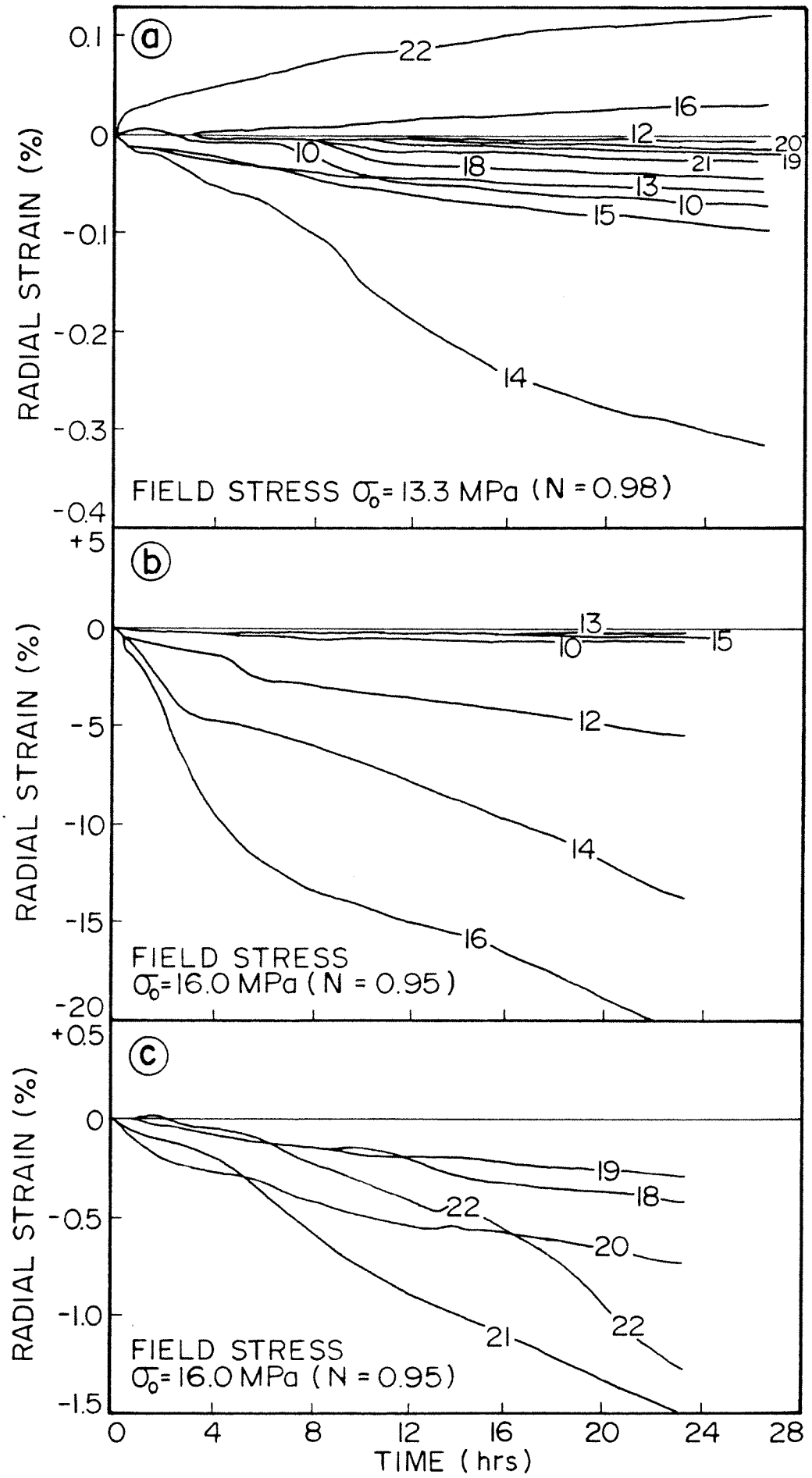

Fig. 5

Kaiser et al., 1984

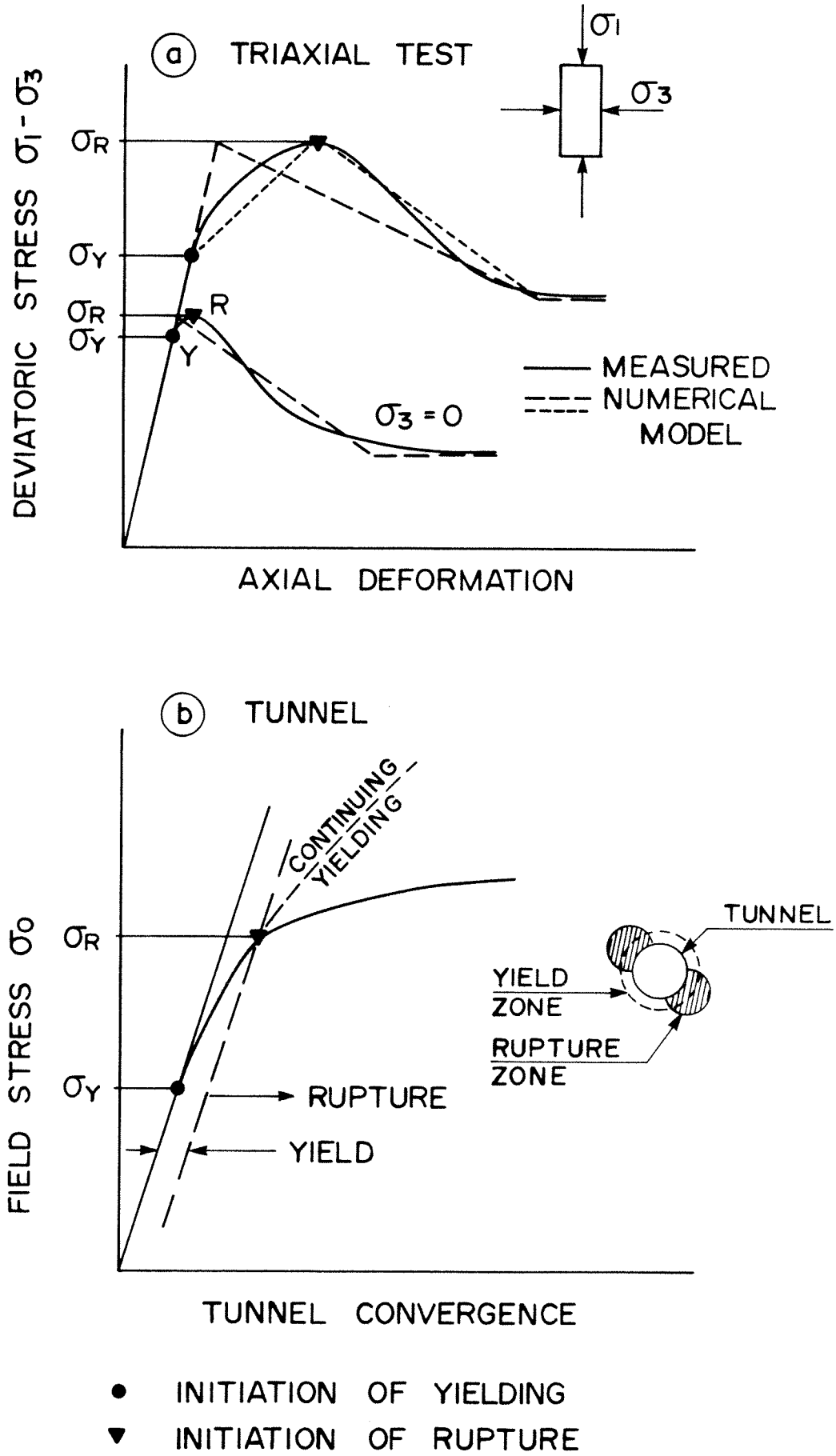

FIG. 6

Kaiser et al., 1984

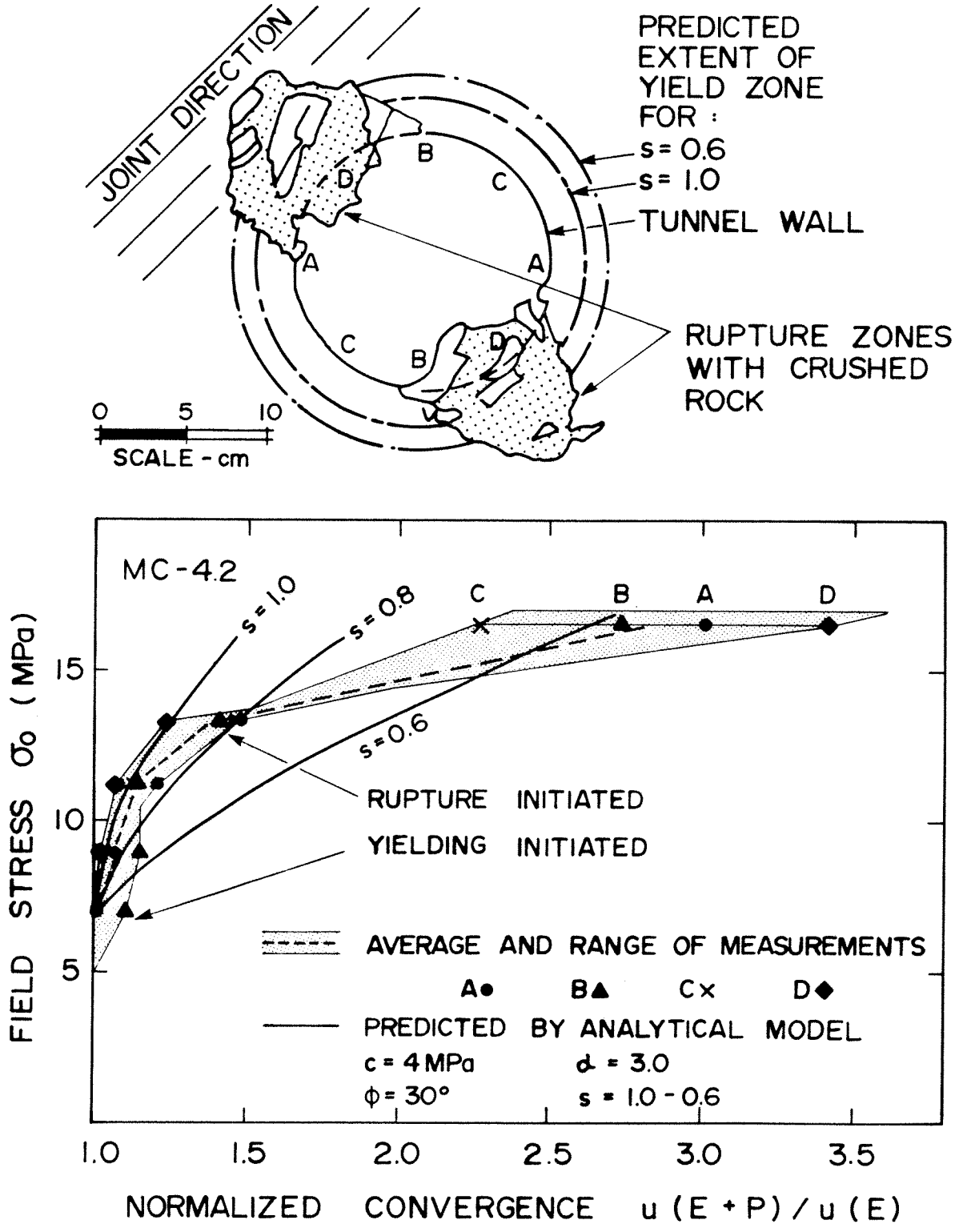

FIG. 7

Kaiser et al., 1984

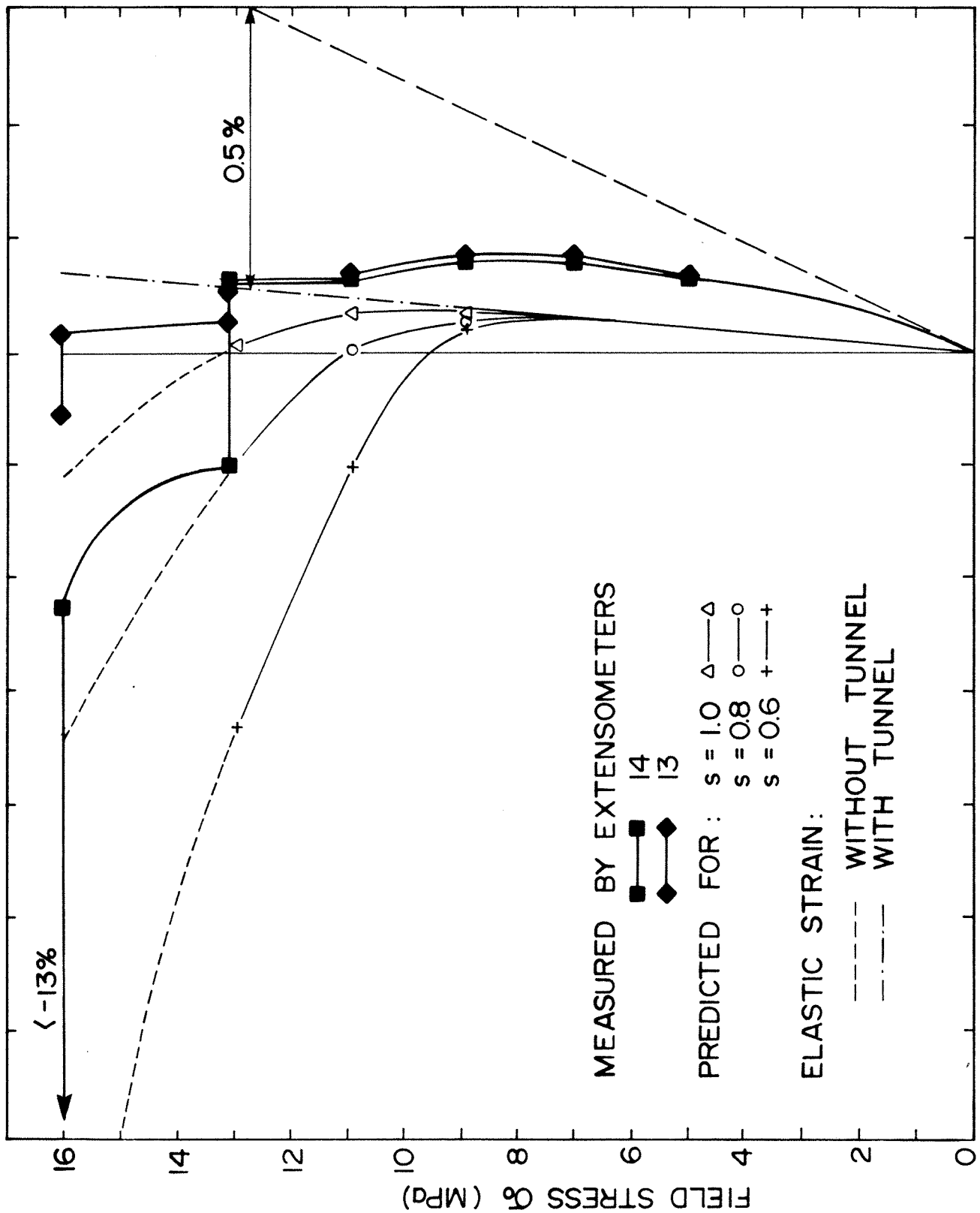

Fig. 8

Kaiser et al., 1984

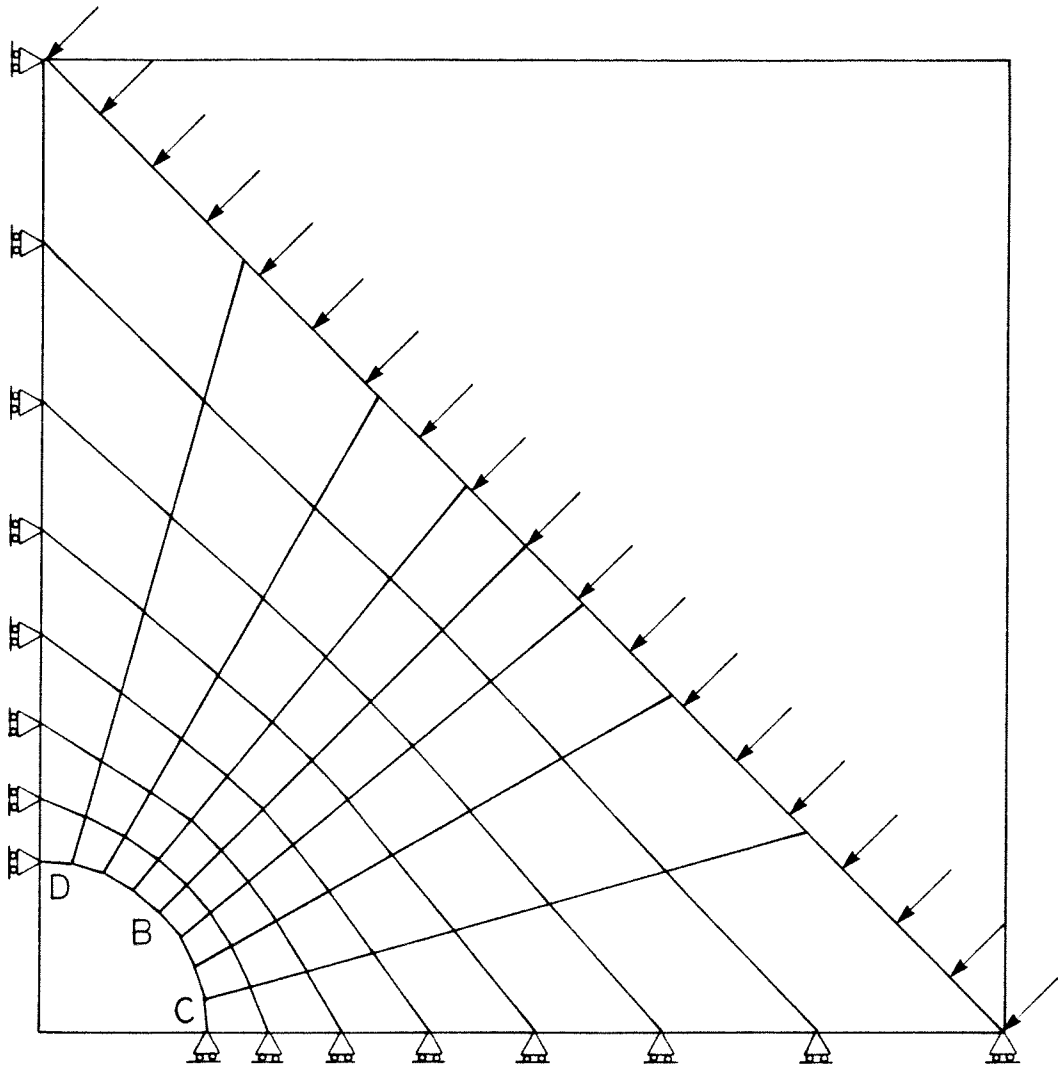

Fig. 9

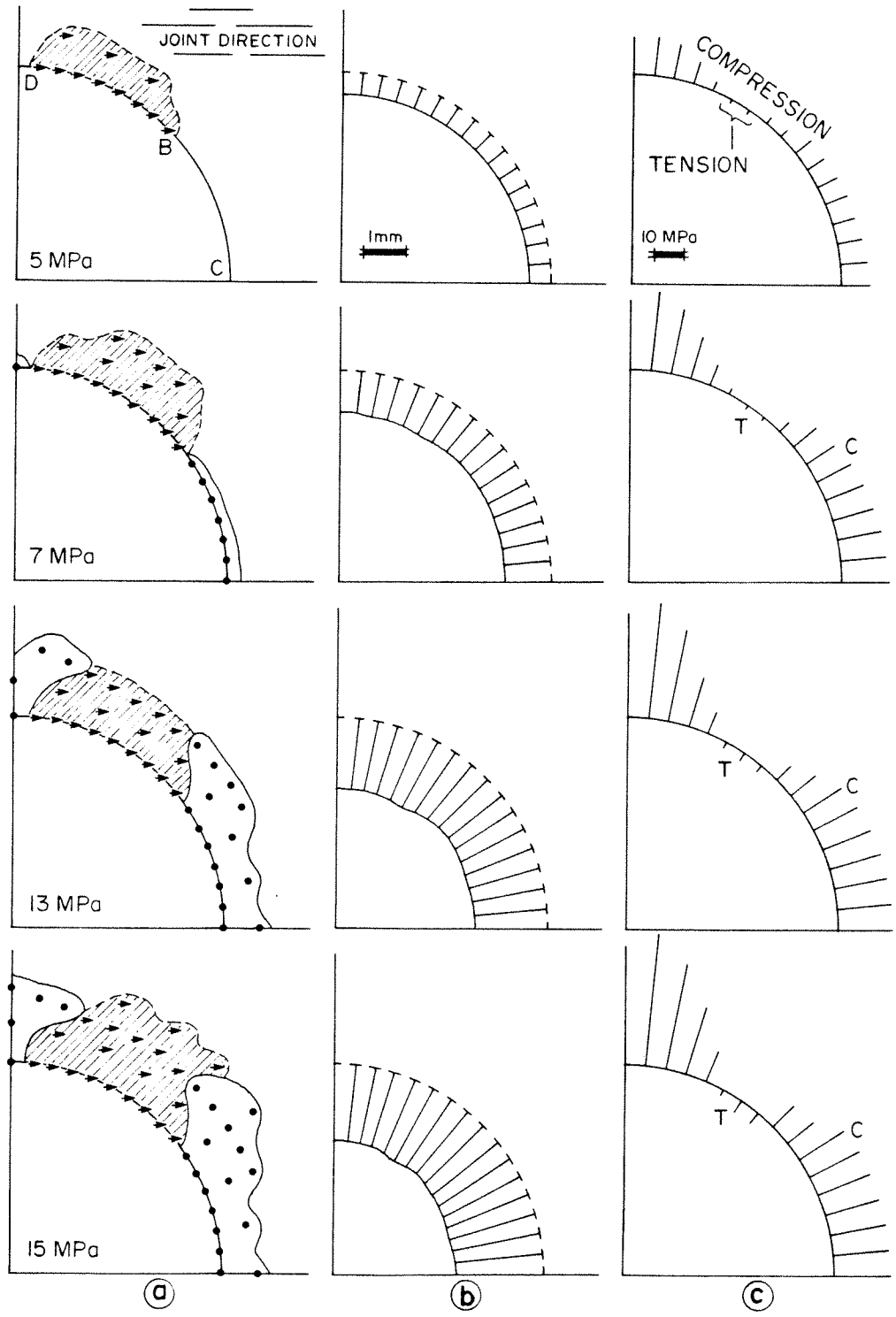

Fig. 10

Kaiser et al., 1984

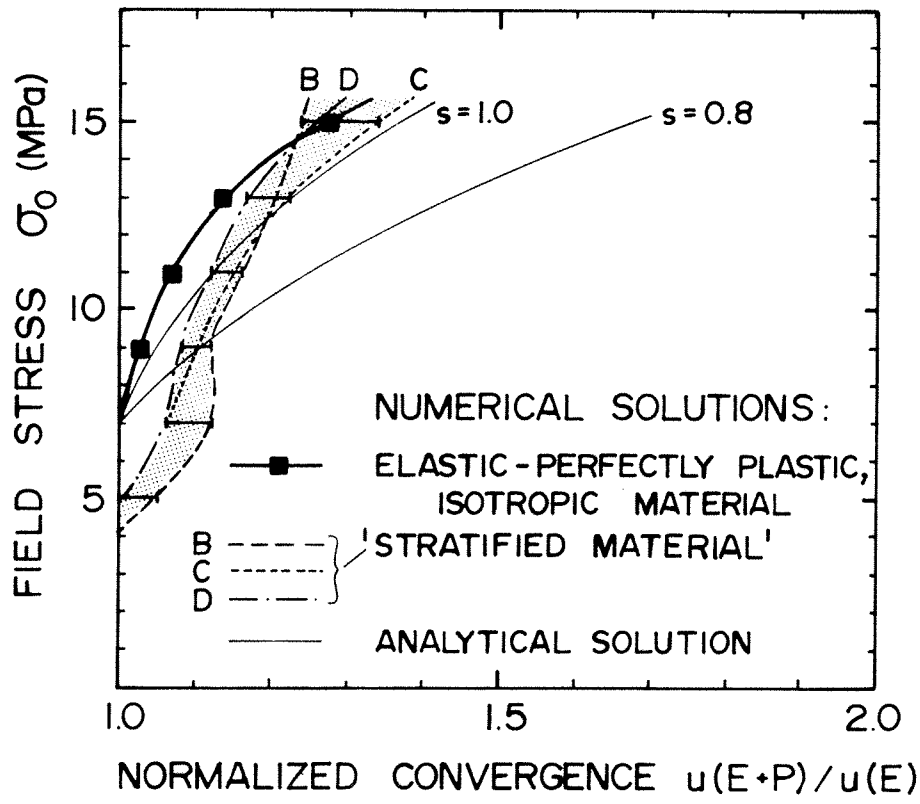

Fig. 11

Kaiser et al., 1984